


ECE/MAE7360. Robust and Optimal Control.

Electrical and Computer Engineering, Utah State University

Project #2: Space-shuttle robustness analysis (stability and performance)


Submit via e-mail only.

1. **Project Objectives: Become expert in doing robustness (stability/performance) analysis using MATLAB mu-synthesis Toolbox.**
2. **System model and sample analysis (see the attached.)**
3. **Required Investigations.**
 - 3.1. Assuming no delay in the actuator delay (refer to page 7-48, the rudder model), repeat all the steps in the space-shuttle robustness analysis (page 7-44 to page 7-74) using the existing given data set. (Note, assume here no delay in both rudder and elevon!)
 - 3.2. Assuming that the natural frequency and the damping factor for BOTH rudder and elevon are all scaled down to 90% of its original value (i.e., $\mathbf{x}_{ele}=0.72*0.90$, $\mathbf{w}_{ele}=14*0.90$ rad/sec. and $\mathbf{x}_{rud}=0.75*0.90$, $\mathbf{w}_{rud}=21*0.90$ rad/sec.), repeat all the steps in the space-shuttle robustness analysis (page 7-44 to page 7-74) using the existing given data set. (Note, we need to include the delay models of both rudder and elevon in this case!)
 - 3.3. Compare three sets of analysis results (original/sample demo, delay removed, and actuator natural frequency/damping factor down-scaled) and make your comments and possible suggestions.

Note:

Project report format:

- (1) A suitable title.
- (2) Introduction of the robustness analysis problem.
- (3) Effect of actuator delay (with vs. without).
- (4) Effect of changes in actuator's damping factor and natural frequency.
- (5) Summary and comments.
- (6) References

Bonus: Make your Project Report self-containing using MS Word or LaTeX.

Attached: A sample robustness analysis. (Extracted from mu-Toolbox User's Guide)

Space Shuttle Robustness Analysis

This section outlines a robust stability and robust performance analysis of the Space Shuttle lateral axis flight control system during re-entry. It serves as a general illustration of the usefulness of the real and complex μ analysis methods.

The system is a simplified model of the Space Shuttle, in the final stages of landing, as it transitions from supersonic to subsonic speeds. The material in this chapter is based on the paper:

Doyle, J., K. Lenz, and A. Packard, "Design Examples Using μ Synthesis: Space Shuttle Lateral Axis FCS During Re-entry," *NATO ASI Series, Modelling, Robustness, and Sensitivity Reduction in Control Systems*, vol. 34, Springer-Verlag, 1987.

The analysis procedure involves several steps:

- 1 Build uncertain model of plant.
- 2 Define performance specifications and uncertainty bounds.
- 3 Construct open-loop interconnection.
- 4 Close feedback loop with controller.
- 5 Perform a variety of real and complex μ analysis tests on the closed-loop system, and explore the impact of the uncertainty model (real vs. complex) on the robust stability and robust performance requirements.
- 6 Construct worst-case perturbations, and see their effect on the closed-loop system in the frequency and time domain.

Aircraft Model: Rigid-Body

The rigid body model for the aircraft at Mach 0.9 is a four-state system, with states

$$x = \begin{bmatrix} \beta \\ p \\ r \\ \phi \end{bmatrix} = \begin{bmatrix} \text{sideslip angle (rad)} \\ \text{roll rate (rad/s)} \\ \text{yaw rate (rad/s)} \\ \text{bank angle (rad)} \end{bmatrix}$$

An input/output block diagram of the aircraft is shown in Figure 7-32.

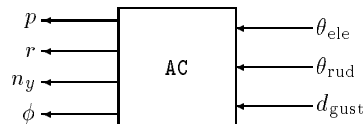


Figure 7-32: Input-Output Description of the Aircraft

The three inputs to the aircraft are denoted by u ,

$$u = \begin{bmatrix} \theta_{ele} \text{ (rad)} \\ \theta_{rud} \text{ (rad)} \\ d_{gust} \text{ (ft/sec)} \end{bmatrix}$$

The first input is the actual angular deflection of the elevon surface. The second is the actual deflection of the rudder surface. Finally, there is a lateral wind gust disturbance input, due to the winds that occur at this altitude.

There are four output variables of the aircraft. Three of these are states, while the fourth is the lateral acceleration at the pilot's location, denoted n_y (units of n_y are ft/sec^2).

$$y = \begin{bmatrix} p \\ r \\ n_y \\ \phi \end{bmatrix}$$

All variables in y are measured with inertial devices (gyroscopes and accelerometers) whose individual noise characteristics are discussed later.

Aircraft Model: Aerodynamic Uncertainty

The major source of uncertainty in the aircraft model (AC) is in the aerodynamic coefficients. These are standard aerodynamic parameters which express incremental forces and torques generated by incremental changes in sideslip, elevon, and rudder angles. This is a linear relationship, expressed as

$$\begin{bmatrix} \text{side force} \\ \text{yawing moment} \\ \text{rolling moment} \end{bmatrix} = \begin{bmatrix} c_{y\beta} & c_{ya} & c_{yr} \\ c_{\eta\beta} & c_{\eta a} & c_{\eta r} \\ c_{l\beta} & c_{la} & c_{lr} \end{bmatrix} \begin{bmatrix} \beta \\ \theta_{\text{ele}} \\ \theta_{\text{rud}} \end{bmatrix}$$

The coefficients $c_{..}$ are typically estimated based on theoretical predictions, numerical calculations, experiments in wind tunnels, and flight tests. At Mach 0.9, the shuttle is in a transonic regime involving a combination of subsonic and supersonic flows. Theoretical, computational, and wind tunnel techniques are inaccurate at this flight condition, so with extremely limited flight data (early in the shuttle program), the coefficient uncertainty for the shuttle model is unusually large.

Uncertainty in these coefficients is modeled as a nominal value, plus a perturbation.

$$\begin{bmatrix} c_{y\beta} & c_{ya} & c_{yr} \\ c_{\eta\beta} & c_{\eta a} & c_{\eta r} \\ c_{l\beta} & c_{la} & c_{lr} \end{bmatrix} = \begin{bmatrix} \bar{c}_{y\beta} & \bar{c}_{ya} & \bar{c}_{yr} \\ \bar{c}_{\eta\beta} & \bar{c}_{\eta a} & \bar{c}_{\eta r} \\ \bar{c}_{l\beta} & \bar{c}_{la} & \bar{c}_{lr} \end{bmatrix} + \begin{bmatrix} r_{y\beta}\delta_{y\beta} & r_{ya}\delta_{ya} & r_{yr}\delta_{yr} \\ r_{\eta\beta}\delta_{\eta\beta} & r_{\eta a}\delta_{\eta a} & r_{\eta r}\delta_{\eta r} \\ r_{l\beta}\delta_{l\beta} & r_{la}\delta_{la} & r_{lr}\delta_{lr} \end{bmatrix}$$

where the values of the $r_{..}$ are

$$\begin{bmatrix} r_{y\beta} & r_{ya} & r_{yr} \\ r_{\eta\beta} & r_{\eta a} & r_{\eta r} \\ r_{l\beta} & r_{la} & r_{lr} \end{bmatrix} = \begin{bmatrix} 2.19 & -1.33 & -0.37 \\ -1.52 & 1.35 & 0.87 \\ -0.72 & 0.52 & 0.24 \end{bmatrix}$$

and the perturbations $\delta_{..}$ are assumed to be fixed, unknown, real parameters, with each satisfying $|\delta_{..}| \leq 1$. We use the notation $r_{..} * \delta_{..}$ to denote the 3×3 perturbation matrix in the model for the aero coefficients, $c_{..}$.

The aircraft model `acnom` has the nominal aerodynamic coefficients absorbed into the state-space data. In addition to the inputs μ and outputs y described earlier, `acnom` has three fictitious inputs and outputs such that the uncertain behavior of the aircraft AC is given by the linear fractional transformation in Figure 7-33.

The state-space model for `acnom` is created by the M-file `mk_acnom`. A listing of state-space model `acnom` is given in “Shuttle Rigid Body Model” at the end of this section.

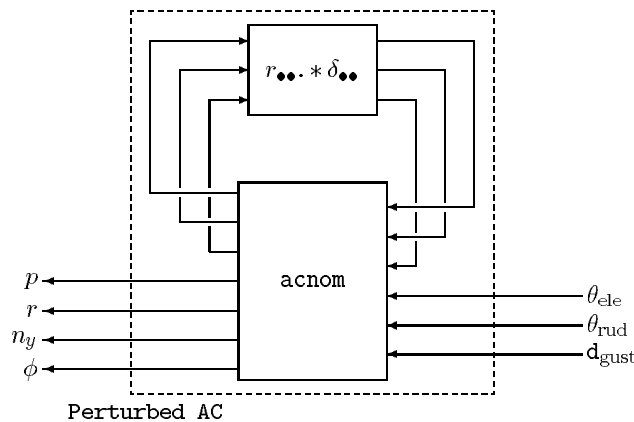
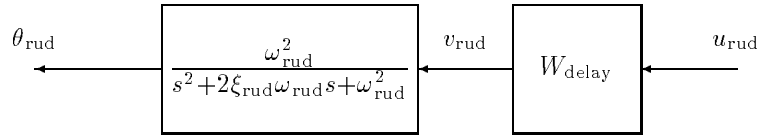


Figure 7-33: Uncertain Aircraft Model

Actuator Models

The aircraft has two controlled inputs, rudder command, and elevon command. Each actuator is modeled with a second order transfer function, as well as a second order delay approximation to model the effects of the digital implementation.

The model for the rudder is



Here, u_{rud} is the electrical command that the controller will generate to move the rudder. The transfer function W_{delay} is a second order approximation of a delay, to model the effects of the digital implementation of the control system. In particular

$$W_{delay}(s) = \frac{1 - 2\xi_{del}(s/\omega_{del}) + (s^2/\omega_{del}^2)}{1 + 2\xi_{del}(s/\omega_{del}) + (s^2/\omega_{del}^2)}$$

with $\omega_{del} = 173$ rad/s, and $\xi_{del} = 0.866$. The transfer function

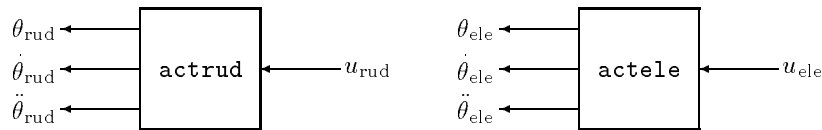
$$\frac{\omega_{rud}^2}{s^2 + 2\xi_{rud}\omega_{rud}s + \omega_{rud}^2}$$

models the physical devices (motors, inertias, etc.) involved in actually moving the rudder. The variable θ_{rud} is the actual deflection of the rudder surface, while u_{rud} represents the command to the rudder system. The values of the parameters are $\xi_{rud} = 0.75$, $\omega_{rud} = 21$ rads/sec.

A similar model is used for the elevon actuation system. The parameters in that case are $\xi_{ele} = 0.72$, $\omega_{ele} = 14$ rads/sec, with an identical second order delay model.

The state-space models for the actuators are created by the M-file `mk_act`. Since the closed-loop performance objectives include penalties on the

deflections, rates, and accelerations of the control surfaces, the state-space models created in `mk_act` each have three outputs, as shown below.



Exogenous Disturbances, Noises, and Commands

There are three sources of exogenous signals:

- Wind gusts
- Sensor noise
- Pilot bank-angle command

In the H_∞ framework, all time domain signals are modeled as the unit ball in L_2 , filtered by problem dependent weighting functions which reflect typically occurring signals in the application. In addition to the L_2 gain, the H_∞ norm also has an interpretation in terms of gain from sinusoids to sinusoids. Now, suppose h represents one of the exogenous signals, and W_h is the associated stable weighting function. Then, the signal h is assumed to be any signal from the set

$$h \in \{W_h \eta_h : \|\eta_h\|_2 \leq 1\}$$

By choosing the form of $W_h(s)$, the spectral content of such signals h can be shaped.

- **Lateral Wind Gusts:** The set of lateral wind gusts is modeled as

$$d_{\text{gust}} \in \left\{ W_{\text{gust}} \eta_{\text{gust}} : W_{\text{gust}} = 30 \frac{1+s/2}{1+s}, \|\eta_{\text{gust}}\|_2 \leq 1 \right\}.$$

The set on the right-hand side of the equation models the typical wind gusts that the shuttle will encounter at this flight condition.

- **Sensor Noise:** Each measurement is corrupted with sensor noise which becomes more severe with increasing frequency. Since p and r are measured with comparable gyroscopes, their sensor noise weights are identical,

$$W_p = W_r = 0.0003 \frac{1 + s/0.01}{1 + s/0.5}$$

These weighting functions imply a low frequency measurement error in p and r of 0.0003 rads/sec, and a high frequency error of 0.015 rads/sec. The model of the measured value of p , denoted p_{meas} , is given by

$$p_{\text{meas}} = p + W_p \eta_p$$

where η_p is an arbitrary signal, with $\|\eta_p\|_2 \leq 1$. This type of weighted, additive L_2 sensor noise is assumed for each of the 4 measured variables.

The measurement of ϕ is obtained from a navigation package at a reduced sample rate, so its weight is chosen to be

$$W_\phi = 0.0007 \frac{1 + s/0.01}{1 + s/2}$$

which is relatively large in the mid-to-high frequency range. The sensor noise weight on the n_y accelerometer is

$$W_{n_y} = 0.25 \frac{1 + s/0.05}{1 + s/10}$$

For the variables r , ϕ , and n_y , we have

$$r_{\text{meas}} = r + W_r \eta_r$$

$$\phi_{\text{meas}} = \phi + W_\phi \eta_\phi$$

$$n_{y_{\text{meas}}} = n_y + W_{n_y} \eta_{n_y}$$

- **Pilot Bank-Angle Command:** In this problem, the pilot (or autopilot) takes the shuttle through a series of sweeping “S” turns to slow the vehicle down.

These require accurate tracking of a bank-angle command. Typical bank-angle commands are modeled as

$$\phi_{\text{cmd}} = W_{\phi_{\text{cmd}}} \eta_{\phi_{\text{cmd}}},$$

where $\eta_{\phi_{\text{cmd}}}$ is assumed to be an arbitrary signal with $\|\eta_{\phi_{\text{cmd}}}\|_2 \leq 1$. In this example, the weight on the bank-angle command is chosen as

$$W_{\phi_{\text{cmd}}} := 0.5 \frac{1 + s/2}{1 + s/0.5}$$

The particular choice roughly implies that the bank-angle commands are dominated by low frequency signals, with a maximum magnitude of approximately 0.5 radians.

The noise weighting functions are denoted by $W_{\text{noise}} = \text{diag}\{W_p, W_r, W_\phi, W_{n_y}\}$ in the control block diagram.

Errors

There are several variables that are to be kept small in the face of the exogenous signals listed in the previous section. In this context, these variables will be considered *errors*.

Actuator signal levels: the angular position, angular rates, and angular accelerations of the rudder (\cdot_{rud}) and elevon (\cdot_{ele}) surfaces should remain reasonably small in the face of the exogenous signals. The signals are weighted to give an actuator error vector of

$$e_{\text{act}} = \begin{bmatrix} e_e \\ e_{\dot{e}} \\ \ddot{e}_e \\ e_r \\ e_{\dot{r}} \\ \ddot{e}_r \end{bmatrix} := \begin{bmatrix} 4 \theta_{\text{ele}} \\ \dot{\theta}_{\text{ele}} \\ 0.005 \ddot{\theta}_{\text{ele}} \\ 2 \theta_{\text{rud}} \\ 0.2 \dot{\theta}_{\text{rud}} \\ 0.009 \ddot{\theta}_{\text{rud}} \end{bmatrix}$$

This performance specification can be loosely interpreted as a requirement that the closed-loop system should, under the excitation of the modeled exogenous signals, maintain θ_{ele} to below 0.25 radians, $\dot{\theta}_{\text{ele}}$ to below 1 rad/sec, $\ddot{\theta}_{\text{ele}}$ to below 200 rads/sec², and so on for the rudder variables. For notational purposes, let W_{act} be the 6×6 constant matrix so that

$$e_{\text{act}} = W_{\text{act}} \begin{bmatrix} \theta_{\text{ele}} \\ \dot{\theta}_{\text{ele}} \\ \ddot{\theta}_{\text{ele}} \\ \theta_{\text{rud}} \\ \dot{\theta}_{\text{rud}} \\ \ddot{\theta}_{\text{rud}} \end{bmatrix}$$

• **Performance variables:**

- The ideal bank angle response (ϕ_{ideal}) of the shuttle to a bank-angle command (ϕ_{cmd}) is

$$\phi_{\text{ideal}} := \frac{1}{1 + 2 \cdot \xi (s/\omega) + (s/\omega)^2} \phi_{\text{cmd}}$$

where $\omega = 1.2$ rad/sec, and $\xi = 0.7$. The bank-angle tracking error is defined as $\phi - \phi_{\text{ideal}}$.

- Turn coordination: in an ideal turn, the bank angle, and the yaw rate are related. For this aircraft, a turn coordination error is defined as

$$r_p := r - 0.037\phi$$

- In a turn, it is desired that the pilot feel very little lateral acceleration, hence, the lateral acceleration variable, n_y , is an error.

These error signals are weighted by frequency dependent weights to give a performance error vector as

$$e_{\text{perf}} := \begin{bmatrix} 0.8 \frac{1+s}{1+s/0.1} & 0 & 0 \\ 0 & 500 \frac{1+s}{1+s/0.01} & 0 \\ 0 & 0 & 250 \frac{1+s}{1+s/0.01} \end{bmatrix} \begin{bmatrix} n_y \\ r - 0.037\phi \\ \phi - \phi_{\text{ideal}} \end{bmatrix}$$

For notational purposes, let W_{perf} be a 3×5 transfer function matrix so that

$$e_{\text{perf}} = W_{\text{perf}} \begin{bmatrix} p \\ r \\ n_y \\ \phi \\ \phi_{\text{ideal}} \end{bmatrix}$$

The error weight on the lateral acceleration indicates a tolerance for low frequency accelerations of 1.25 ft/sec^2 , which is relaxed at high frequency, allowing accelerations up to 12.5 ft/sec^2 . Again, these specifications correspond to n_y errors produced by the exogenous signal set (wind gusts, measurement noises, and bank angle commands). Similar interpretation is given to the other performance variables.

LFT Aero-Coefficient Uncertainty

The perturbations in the aero-coefficients can be written as an LFT (linear fractional transformation) on a structured uncertainty matrix. Define constant matrices $W_L \in \mathbf{R}^{3 \times 9}$ and $W_R \in \mathbf{R}^{9 \times 3}$ such that

$$W_L \cdot \text{diag}[\delta_{y\beta}, \delta_{\eta\beta}, \delta_{l\beta}, \delta_{ya}, \dots, \delta_{lr}] \cdot W_R = \begin{bmatrix} r_{y\beta} \delta_{y\beta} & r_{ya} \delta_{ya} & r_{yr} \delta_{yr} \\ r_{\eta\beta} \delta_{\eta\beta} & r_{\eta a} \delta_{\eta a} & r_{\eta r} \delta_{\eta r} \\ r_{l\beta} \delta_{l\beta} & r_{la} \delta_{la} & r_{lr} \delta_{lr} \end{bmatrix}$$

for all $\delta \dots$. This is easily done with the permutation matrices W_L and W_R shown below.

$$W_R^T = \begin{bmatrix} 1 & 1 & 1 & 0 & 0 & 0 & 0 & 0 & 0 \\ 0 & 0 & 0 & 1 & 1 & 1 & 0 & 0 & 0 \\ 0 & 0 & 0 & 0 & 0 & 0 & 1 & 1 & 1 \end{bmatrix}$$

$$W_L = \begin{bmatrix} 2.19 & 0 & 0 & -1.33 & 0 & 0 & -0.37 & 0 & 0 \\ 0 & -1.52 & 0 & 0 & 1.35 & 0 & 0 & 0.87 & 0 \\ 0 & 0 & -0.72 & 0 & 0 & 0.52 & 0 & 0 & 0.24 \end{bmatrix}$$

Create Open-Loop Interconnection

The aircraft model, actuator models, and weighting functions discussed in the previous sections can be constructed from M-files.

```
mk_acnom;  
mk_act;  
mk_wts;
```

The open-loop interconnection structure, which includes the uncertainty model and the performance objectives, is shown in Figure 7-34.

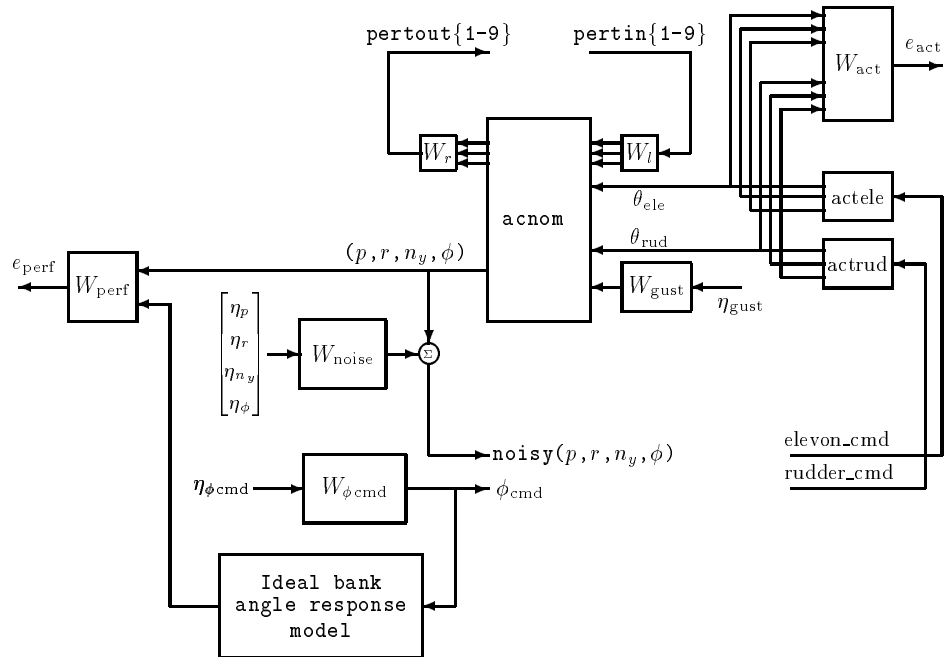


Figure 7-34: Shuttle Interconnection Structure

The M-file `mk_olic` uses the `sysic` command to create a `SYSTEM` matrix description of the open-loop interconnection structure. In the workspace, the open-loop system is denoted by `olic`, and has 23 states, 23 outputs, and 17 inputs.

```
mk_olic;
minfo(olic)
```

A schematic diagram, with the specific input/output ordering for `olic`, is shown in Figure 7-35.

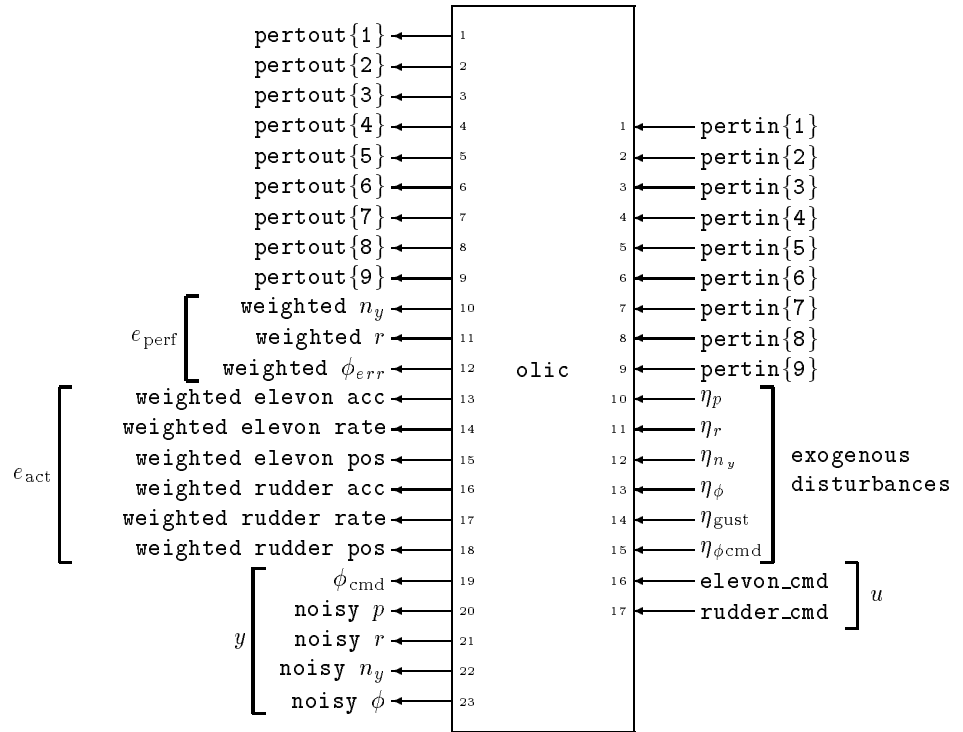
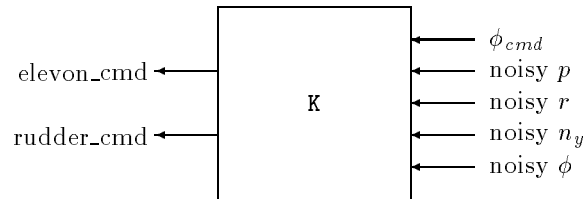


Figure 7-35: Schematic Diagram of Space Shuttle olic

Controllers

In this section, the robustness properties of three different controllers are analyzed using μ . The controllers receive four sensor measurements along with the ϕ command signal and produce two control signals for the elevon and rudder commands. The controller block diagram is shown below.



In this example, each controller has different characteristics:

- k_h is designed to optimize H_∞ performance, under the assumption that there is no model uncertainty;
- k_μ is designed with the $D - K$ iteration approach to μ -synthesis;
- k_x is constructed to be a tradeoff between the two controllers

The μ -Tools commands to design the H_∞ optimal controller, k_h , are:

```
olic_h = sel(olic,[10:23],[10:17]);
minfo(olic_h)
k_h = hinfsyn(olic_h,5,2,0,5,0.1);
```

The first command, `sel`, removes the aero-coefficient uncertainty channels, leaving only the exogenous signals and errors, and feedback signals. The third command, `hinfsyn`, designs a suboptimal H_∞ controller for the open-loop system `olic_h`. This controller measures five signals, and generates two control signals.

It is simple to check some characteristics of the controller and the closed-loop system

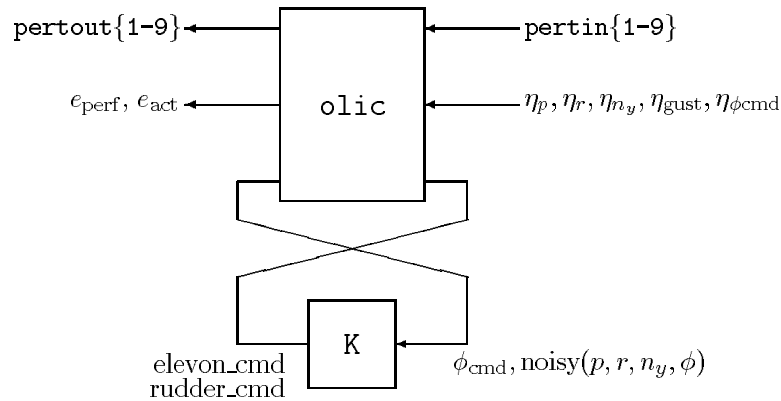
```
minfo(k_h)
clp_h = starp(olic,k_h,5,2);
rifd(spoles(clp_h))
rifd(spoles(k_h))
```

The two other controllers have already been designed and stored in the file `shutcont.mat`.

```
load shutcont
minfo(k_x)
minfo(k_mu)
```

Nominal Frequency Responses

The closed-loop system is constructed using the star product command `starp`.



In the closed-loop system, there are six exogenous signals (the six η signals: four sensor noises, wind gust, bank angle command) and nine errors (weighted performance error vector and the weighted actuator error vector). The nominal performance objective is that this multivariable transfer function matrix should have an H_∞ norm less than 1. Using μ -Tools, it is easy to evaluate this performance criterion. Simply form the closed-loop system, calculate its frequency response, and plot the norm of the appropriate transfer function versus frequency.

```

omega = logspace(-2,3,30);
clp_h = starp(olic,k_h,5,2);
clp_hg = frsp(clp_h,omega);
clp_x = starp(olic,k_x,5,2);
minfo(clp_x)
clp_xg = frsp(clp_x,omega);
minfo(clp_xg)
clp_mu = starp(olic,k_mu,5,2);
clp_mug = frsp(clp_mu,omega);

```

Note that the closed-loop systems have additional inputs and outputs from the nine aero-perturbation channels. The relevant exogenous signals and errors are selected (using `sel`) before calculating the maximum singular value (`vnorm`).

```

np_hg = sel(clp_hg,[10:18],[10:15]);
np_xg = sel(clp_xg,[10:18],[10:15]);
np_mug = sel(clp_mug,[10:18],[10:15]);
vplot('liv,m',vnorm(sel(clp_hg,10:18,10:15)),...
      vnorm(sel(clp_xg,10:18,10:15)),...
      vnorm(sel(clp_mug,10:18,10:15)))
title('NOMINAL PERFORMANCE: ALL CONTROLLERS')

```

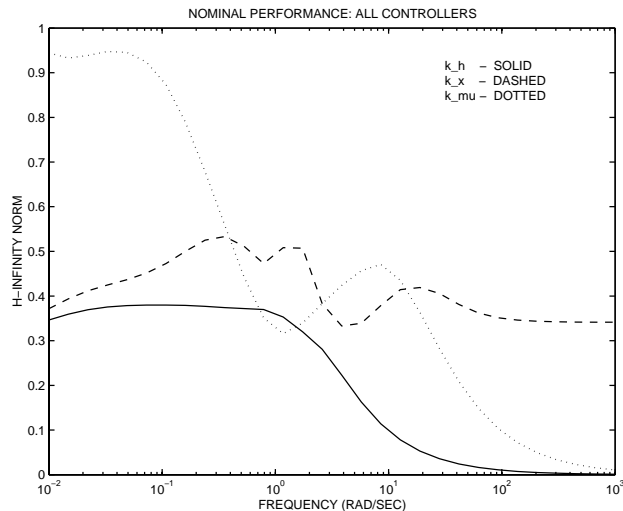


Figure 7-36: Nominal Performance of k_h , k_x , and k_μ

Note that the best nominal performance is achieved by controller k_h , as seen in Figure 7-36. This is not surprising, since it was designed specifically with these disturbances and errors in mind. Relatively, the performance from k_μ is poor, though it does meet the nominal performance objective. In later calculations, it will become clear that the degradation in nominal performance is offset by a much greater insensitivity to variations in the aerodynamic coefficients.

Robust Stability

Using μ , the robust stability characteristics of each closed-loop system can be evaluated. The uncertain parameters ($\delta_{j\beta}, \dots, \delta_{I_r}$) can be assumed to be real, representing uncertainty in the constant aerodynamic coefficients. However, the flow around the vehicle is very complex, and the quasi-steady implication of constant aerodynamic coefficients is somewhat simplistic. Consequently, for a more conservative analysis, the uncertain parameters can be treated as complex. In this section, both models of uncertainty will be analyzed, and compared. Refer to Chapter 4, “Modeling and Analysis of Uncertain Systems” for more detail on the interpretations.

This motivates two separate representations of the uncertainty set,

$$\Delta_{\mathbf{C}} := \{\text{diag}[\delta_1, \delta_2, \dots, \delta_9] : \delta_i \in \mathbf{C}\}$$

$$\Delta_{\mathbf{R}} := \{\text{diag}[\delta_1, \delta_2, \dots, \delta_9] : \delta_i \in \mathbf{R}\}$$

where the perturbations represent uncertainty in the aero-coefficients. Note that the first set contains all complex perturbations, while the second set includes only real perturbations.

In the μ -Tools syntax, these are represented as

```
delsetrs_C = ones(9,2);
delsetrs_R = [-ones(9,1) zeros(9,1)];
```

Here, the lower case rs refers to robust stability (as opposed to robust performance, rp, which will be addressed later).

The perturbation inputs/outputs from the frequency responses are selected for a robust stability μ test. The input/output channels associated with the performance criterion are not used in the robust stability μ test. A diagram of the closed-loop system is shown in Figure 7-37.

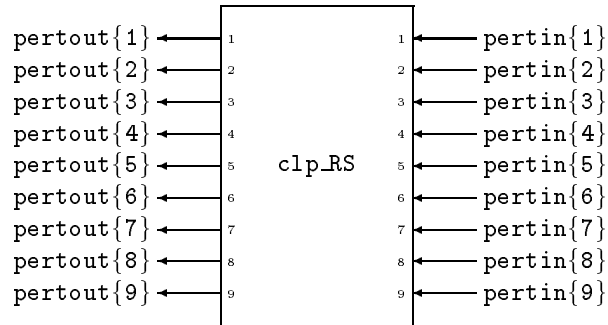


Figure 7-37: Schematic Design of clp_RS

```
clp_hgRS = sel(clp_hg,1:9,1:9);
clp_xgRS = sel(clp_xg,1:9,1:9);
clp_mugRS = sel(clp_mug,1:9,1:9);
```

Calculate μ across frequency, and look at μ plots. Start with the complex uncertainty structure.

```
[bnds_h,dv_h,sens_h,rp_h]=mu(clp_hgRS,delsetrs_C);
[bnds_x,dv_x,sens_x,rp_x]=mu(clp_xgRS,delsetrs_C);
[bnds_mu,dv_mu,sens_mu,rp_mu]=mu(clp_mugRS,delsetrs_C);
vplot('liv,d',bnds_h,'-',bnds_x,'--',bnds_mu,'-.')
title('ROBUST STABILITY OF CLOSED-LOOP: COMPLEX')
```

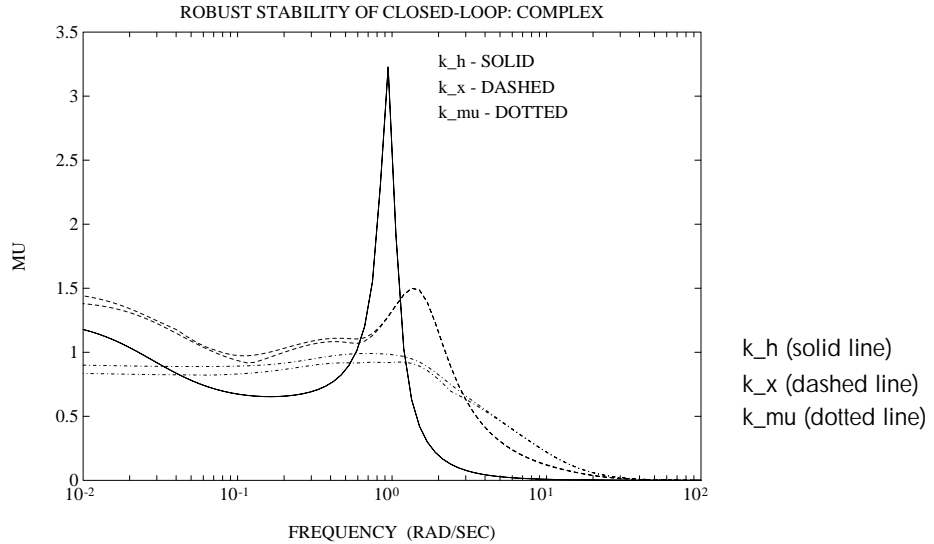


Figure 7-38: Complex Robust Stability μ Analysis of k_h , k_x , and k_{μ}

According to Figure 7-38, the k_{μ} controller has the best robust stability properties when the perturbations are treated as complex (dynamic). The peak of the lower bound, 0.9, implies that there is a diagonal complex perturbation of size, $\frac{1}{0.9}$, that causes instability. The peak of the upper bound, approximately 0.99, implies that for diagonal perturbations smaller than $\frac{1}{0.99}$, the closed-loop system remains stable. The gap between the upper and lower bound can be reduced by using the “c” option in the μ command. Without this option, the upper bound from μ is a computational approximation to

$$\inf_{D \in \mathbf{D}} \bar{\sigma}(DMD^{-1})$$

that can be refined (option “c”) at the expense of slower execution. Using the “c” option reduces the upper bound peak to 0.9, so that the complex μ analysis gives a tight estimate on the size of the smallest destabilizing perturbation.

Similar interpretations are possible for the closed-loop systems with controllers k_h and k_x , though, since the μ plots have larger peaks, the bound on allowable perturbations is smaller. Hence, the closed-loop system with the

controller k_{μ} achieves robust stability to complex perturbations, whereas the other controllers do not.

The closed-loop system is also analyzed treating the aerodynamic uncertainty as real perturbations with the μ -Tools `mu` command.

```
[rbnds_h,rrp_h] = mu(clp_hgRS,delsetrs_R);
[rbnds_x,rrp_x] = mu(clp_xgRS,delsetrs_R);
[rbnds_mu,rrp_mu] = mu(clp_mugRS,delsetrs_R);
vplot('liv,d',[rbnds_h,'- ',rbnds_x,'- - ',rbnds_mu,'- . .'])
title('ROBUST STABILITY OF CLOSED-LOOP: REAL')
```

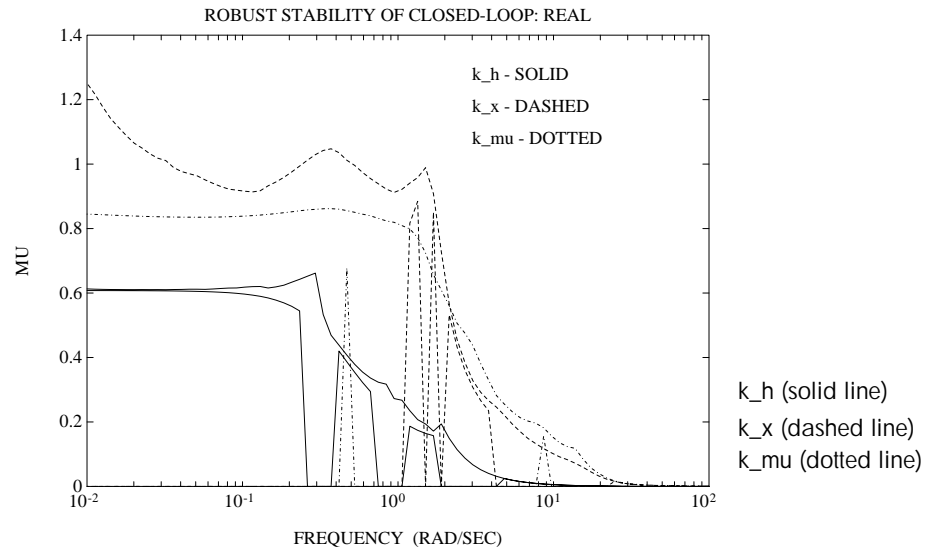


Figure 7-39: Real Robust Stability μ Analysis of k_h , k_x , and k_{μ}

The k_h controller has the best robust stability properties, when the perturbations are treated as real, as seen in Figure 7-39. This is in contrast to the robust stability analysis with complex perturbation where k_{μ} exhibited the best properties. The peak of the upper bound, approximately 0.66, implies that for diagonal, real perturbations smaller than $\frac{1}{0.66}$, the closed-loop system remains stable. The lower bound in Figure 7-39 is often 0 and does not converge for all values of frequency, leading to a large gap between the upper and lower bound. This gap can be reduced by adding a small amount of complex perturbation to the pure real perturbation. A detailed discussion of this

approach can be found in the “Mixed Real/Complex Structured Singular Value” section in Chapter 4.

Robust Performance

Using μ , the robust performance characteristics of each closed-loop system can be evaluated. The uncertain parameters are treated as real parameters in this analysis. These parameters can also be treated as complex perturbations, though this is not done in this section.

The appropriate block structure for the robust performance test is

$$\Delta_P := \{\text{diag}[\delta_1, \delta_2, \dots, \delta_9, \Delta_{10}] : \delta_i \in \mathbf{R}, \Delta_{10} \in \mathbf{C}^{6 \times 9}\}$$

which is simply an augmentation of the original real robust stability uncertainty set, Δ_R , with a complex 6×9 full block to include the performance objectives. Recall from the “Using m to Analyze Robust Performance” section in Chapter 4: H_∞ performance objectives are always represented with a full, complex block. Hence,

$$\text{delsetrp}_R = [\text{delsetrs}_R; 6 \ 9]$$

The μ calculations are performed on the entire 18×15 closed-loop matrix, which includes the perturbation channels and the exogenous signals and errors. The command `mu` is called with both real and complex blocks.

```
[bnds_h,ph] = mu(clp_hg,delsetrp_R);  
[bnds_x,px] = mu(clp_xg,delsetrp_R);  
[bnds_mu,p_mu] = mu(clp_mug,delsetrp_R);  
vplot('liv,d',bnds_h,'-',bnds_x,'--',bnds_mu,'-.')  
title('ROBUST PERFORMANCE OF ALL CONTROLLERS')
```

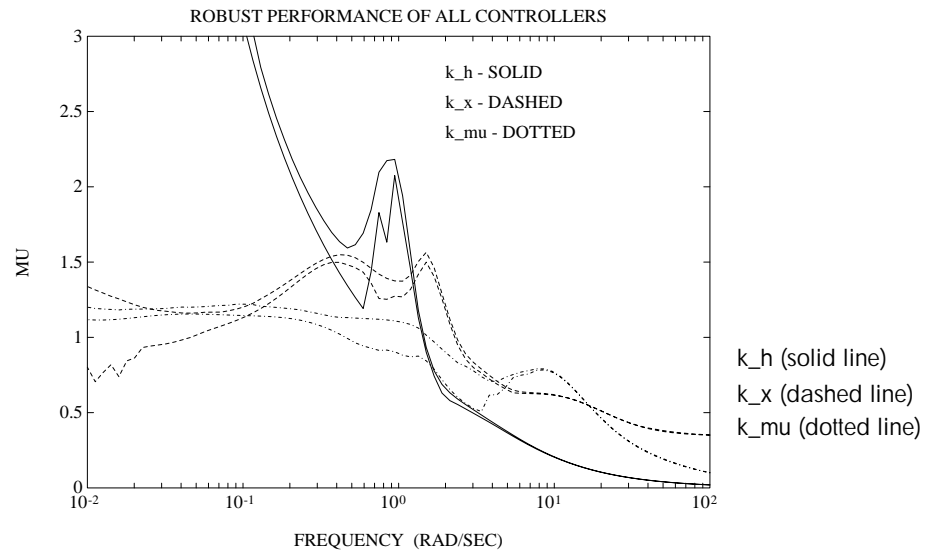


Figure 7-40: Robust Performance μ Plots of k_h , k_x , and k_{μ}

The axis is selected in Figure 7-40 to show a comparison of controllers k_x and k_{μ} . At low frequency, the closed-loop robust performance with k_h implemented gets as bad as 14. The closed-loop system using controller k_x achieves a robust performance μ value of 1.56, while controller k_{μ} achieves a robust performance μ value of 1.22.

Worst-case Perturbations

Using a μ calculation, we have seen that all controllers achieve robust-stability to the 9×9 real uncertainty matrix which represents uncertainty in the aero-coefficients. However, the performance of each closed-loop system degrades differently under LFT real, diagonal perturbations. We use `wcperf` to compute the worst-case performance degradation as well as the worst-case, norm 1, perturbation. The worst-case perturbation of norm 1 will be used in the next section for uncertain time-domain simulations.

```
[deltabadh,wcp_lowh,wcp_upph] = wcperf(clp_hg,delsetrs_R,.05,4);
[deltabadx,wcp_lowx,wcp_uppx] = wcperf(clp_xg,delsetrs_R,.05,10);
[deltabadmu,wcp_lowmu,wcp_uppmu]= wcperf(clp_mug,delsetrs_R,.05,10);
vplot(wcp_lowh,wcp_upph,wcp_lowx,wcp_uppx,wcp_lowmu,wcp_uppmu)
```

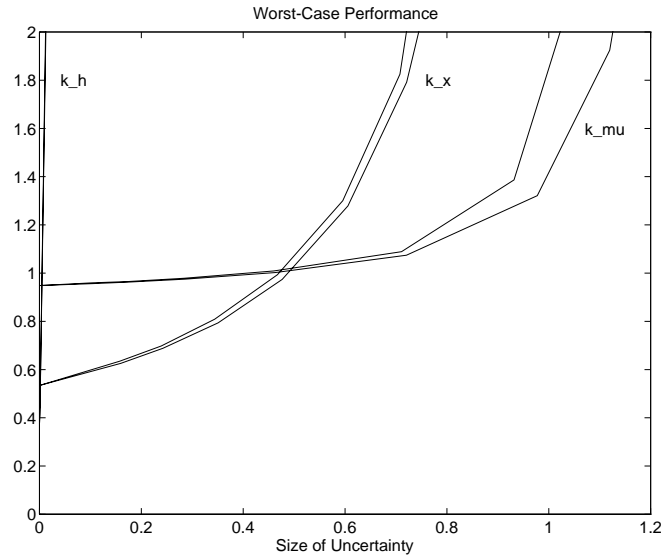


Figure 7-41: Performance Degradation of Closed-Loop

Using k_h , it is clear that the closed-loop performance degrades rapidly and severely. It would not be an acceptable controller in the real aircraft.

Note Optimizing the H_∞ norm of some closed-loop transfer function *does not, in any way, guarantee robustness* to perturbations at other points in the feedback loop.

Using k_x and k_μ , reasonable robustness properties (on the order of the original specifications) are attained. The controller k_x achieves better nominal performance (i.e., at $\|\Delta\| = 0$), at the expense of more rapid potential performance degradation under uncertainty. Both closed-loop systems potentially degrade to unacceptable (performance norm > 1) performance with less than one-half of the original modeled uncertainty. At that level of uncertainty, the closed-loop system with k_μ degrades more gracefully. This type of tradeoff curve illustrates some of the differences between the two controllers, and can be helpful in understanding the tradeoffs involved.

Time Simulations

The open-loop simulation interconnection, Figure 7-42, is similar to `olic`, but contains none of the weighting functions. It is used exclusively for nominal and perturbed time-domain simulations, where unweighted time signals will be calculated and plotted.

```
mk_olsim;
minfo(olsim)
```

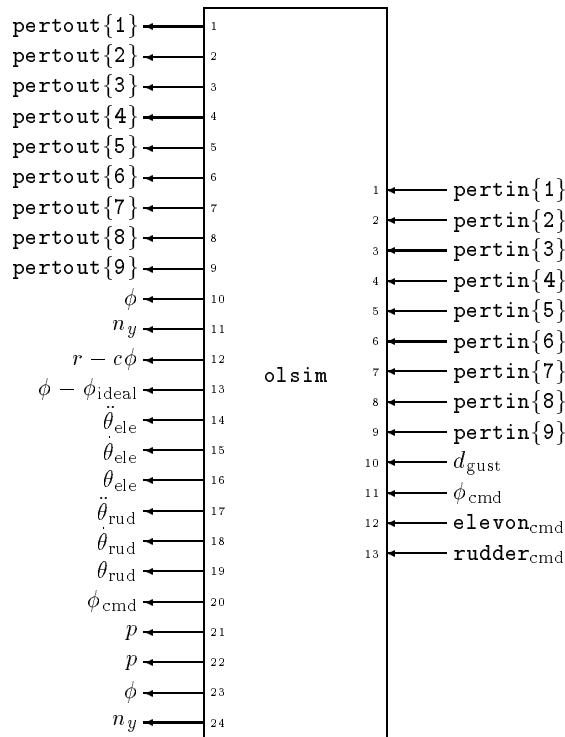


Figure 7-42: Open-Loop Simulation Model

For the purposes of this exercise, the four sensor noises have been eliminated from the simulation model. It is easy to modify `mk_olsim.m` to include these if desired.

The LFT time simulation GUI, `simgui`, is used to simulate the nominal and perturbed time response of the three controllers. For more details on `simgui`

see the “LFT Time Simulation User Interface Tool: simgui” section in Chapter 6.

The main performance objective is bank angle tracking, so the response to a 0.5 radian step input for ϕ_{cmd} is investigated. The gust input is set to zero in these simulations. This data is entered into the simgui Main window Input Signal editable text. Note that ϕ_{cmd} is the 11th input of `olsim` and the second non-perturbation input. The output signals of interest are ϕ , n_y , $r - c\phi$, and $\phi - \phi_{ideal}$, which are outputs 10 through 13 of `olsim` or the first through fourth outputs after the perturbation has been included. In the simgui Main window, input `olsim` into the Plant editable text. Figure 7-43 shows the main simulation window for the nominal and perturbed response of controller k_x .

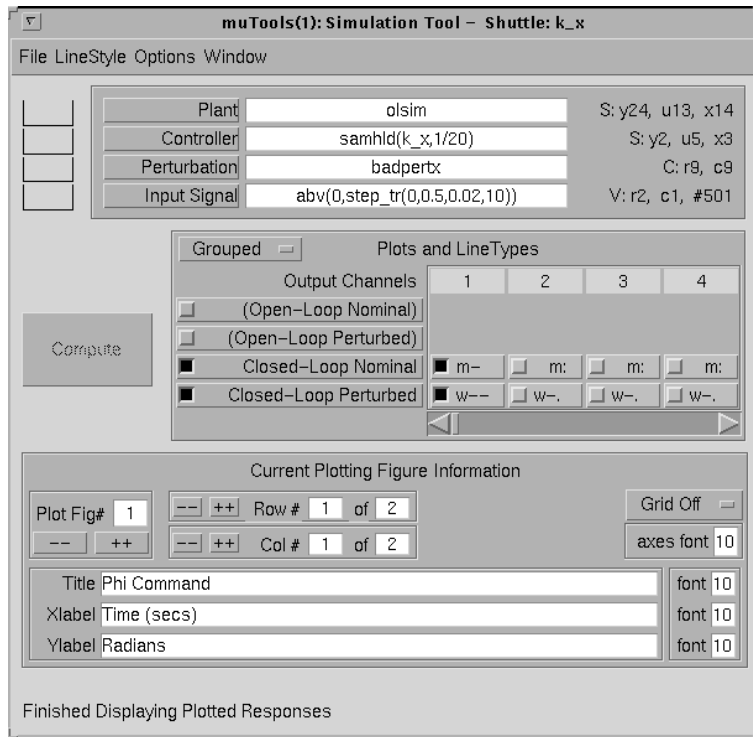


Figure 7-43: simgui Main Window for Shuttle Time Simulation

We are interested in the nominal and perturbed closed-loop response in the presence of a worst-case, real perturbation. This corresponds to the top nine channels of `olsim`, the aero-coefficient perturbations. Therefore, worst-case real perturbations of size 1 in the aero-coefficients for `k_x` and `k_mu` are calculated using the `wcperfc` command. These perturbations are:

$$\begin{aligned} \text{badpertz} &= \text{diag}([1 \quad 1 \quad 1 \quad -.87 \quad 1 \quad 1 \quad -.28 \quad -1 \quad -1 \quad]) \\ \text{badpertzmu} &= \text{diag}([-1 \quad -1 \quad -1 \quad 1 \quad 1 \quad 1 \quad -1 \quad -1 \quad -1 \quad]) \end{aligned}$$

`badpertz` is used in the perturbed response for controller `k_x` and `badpertzmu` is used as the worst-case real perturbation for controllers `k_h` and `k_mu`. This data is input into the Perturbation editable text in the `simgui` main window.

The controllers are implemented in discrete-time at a sample-rate of 20Hz on the shuttle. To replicate the same implementation, a sample-data time simulation is performed. This simulation is available under the **Options** menu in the Main simulation window. Therefore, the continuous-time controllers, `k_x`, `k_h`, and `k_mu`, must be discretized for the sampled-data time simulation. The continuous-time plant, `olsim`, is simulated at 200Hz and the controllers at 20Hz as seen in the `simgui` parameter window, Figure 7-44.

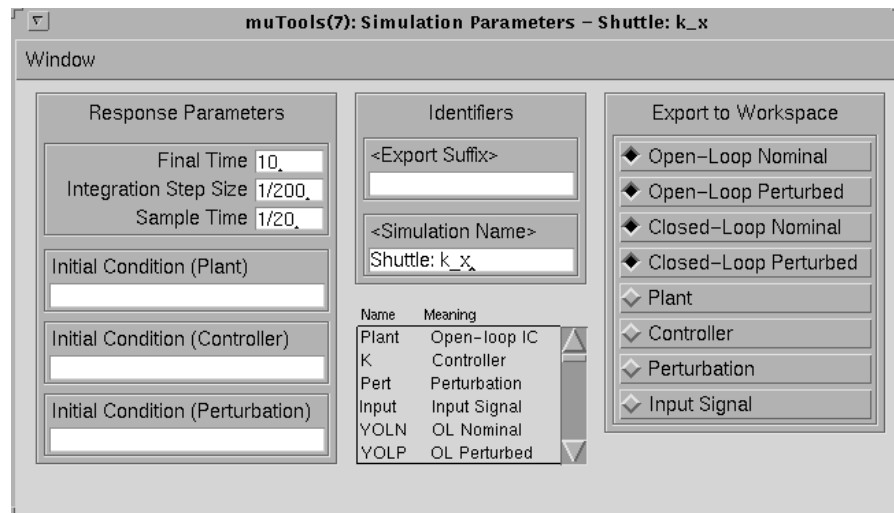
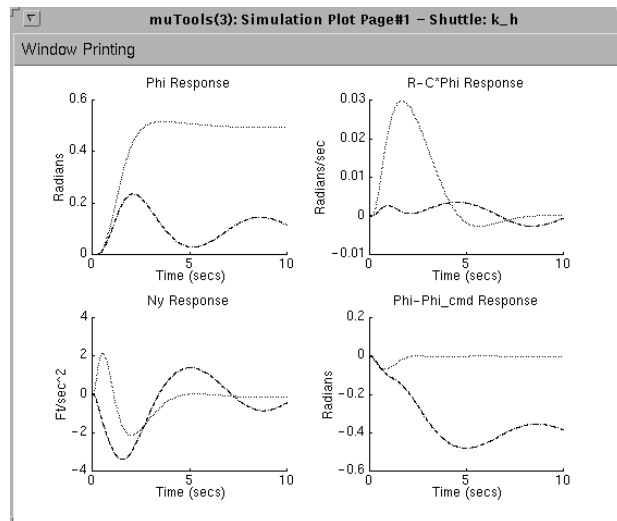
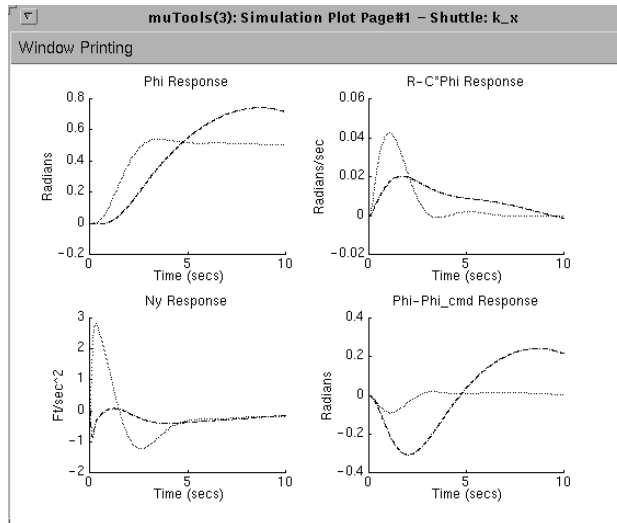


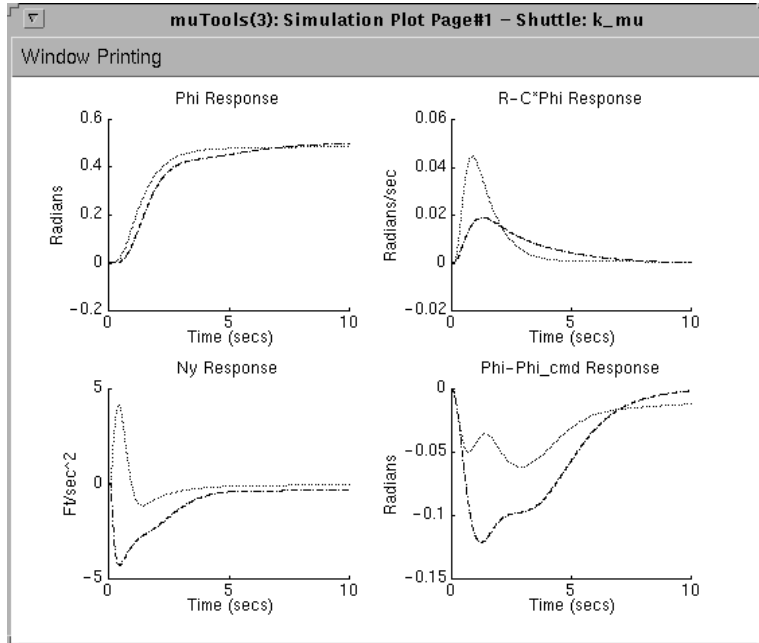
Figure 7-44: `simgui` Parameter Window for Shuttle Time Simulation

The nominal and perturbed closed-loop responses with k_x , k_h , and k_μ implemented are shown in Figure 7-45 and 7-46. As expected, the time domain simulations reinforce the conclusions that were reached in the frequency domain analysis. The nominal performance associated with k_h is superb, but degrades significantly with the aerodynamic uncertainty. In that respect, the controller k_μ performs the best, nearly achieving all of the robust performance objectives. The nominal and perturbed time response of other performance variables can also be easily investigated.



nominal (solid line) perturbed (dashed line)

Figure 7-45: Closed-Loop Nominal and Perturbed Time Response, k_x (top) and k_h



Nominal (solid line) Perturbed (dashed line)

Figure 7-46: Closed-Loop Nominal and Perturbed Time Response, k_{μ}

Conclusions

This exercise illustrated the use of the μ -Tools software to analyze the robust stability and robust performance objectives on a complicated, uncertain plant model.

There is an important feature of the μ software that cannot be overlooked or overemphasized. These algorithms calculate both upper *and* lower bounds for μ , and produce worst-case perturbations which provide the lower bound. The perturbations, and their effects, can be analyzed in both the frequency domain and time domain. In practice, the bad perturbations are also used in high fidelity, nonlinear simulations of the closed-loop system to discover limitations and unforeseen problems.

Although this problem did not have repeated uncertain parameters (each $\delta_{..}$ appeared only once), the algorithms and software do handle these cases, and the reader is referred back to the “Complex Structured Singular Value” section in Chapter 4 for details.

Space Shuttle References

Doyle, J., K. Lenz, and A. Packard, “Design Examples Using μ Synthesis: Space Shuttle Lateral Axis FCS During Reentry,” *NATO ASI Series, Modelling, Robustness, and Sensitivity Reduction in Control Systems*, vol. 34, Springer-Verlag, 1987.

Shuttle Rigid Body Model

The perturbed, state-space rigid body model of the aircraft, *acnom*, is shown in the following figure.

$$\text{acnom} = \begin{bmatrix} \text{A_acnom} & \text{B_acnom} \\ \text{C_acnom} & \text{D_acnom} \end{bmatrix}$$

$$\text{A_acnom} = \begin{bmatrix} -9.5e-2 & 1.4e-1 & -9.9e-1 & 3.6e-2 \\ -3.6e+0 & -4.3e-1 & 2.8e-1 & 0 \\ 4.0e-1 & -1.3e-2 & -8.1e-2 & 0 \\ 0 & 1 & -1.4e-1 & 0 \end{bmatrix}$$

$$\text{B_acnom} = \begin{bmatrix} 1.3e-2 & 0 & 0 & -1.2e-2 & 1.0e-2 & -1.1e-7 \\ 0 & -3.1e-2 & -3.1e+0 & 6.6e+0 & 1.3e+0 & -4.1e-6 \\ 0 & -1.9e-1 & -6.4e-2 & 3.8e-1 & -2.6e-1 & 4.5e-7 \\ 0 & 0 & 0 & 0 & 0 & 0 \end{bmatrix}$$

$$\text{C_acnom} = \begin{bmatrix} 1 & 0 & 0 & 0 \\ 0 & 0 & 0 & 0 \\ 0 & 0 & 0 & 0 \\ 0 & 1 & 0 & 0 \\ 0 & 0 & 1 & 0 \\ -6.8e+1 & -1.7e+0 & -4.1e+0 & -3.7e-5 \\ 0 & 0 & 0 & 1.0e+0 \end{bmatrix}$$

$$\text{D_acnom} = \begin{bmatrix} 0 & 0 & 0 & 0 & 0 & 1.2e-6 \\ 0 & 0 & 0 & 1 & 0 & 0 \\ 0 & 0 & 0 & 0 & 1 & 0 \\ 0 & 0 & 0 & 0 & 0 & 0 \\ 0 & 0 & 0 & 0 & 0 & 0 \\ 1.1e+1 & -1.1e+1 & -1.1e+1 & 2.7e+1 & -3.0e+0 & -7.8e-5 \\ 0 & 0 & 0 & 0 & 0 & 0 \end{bmatrix}$$